CVJ CLUJ VETERINARY JOURNAL

Article

Histopathological Evaluation of Experimentally Induced Volumetric Muscle Loss in Rats

Andreea-Alina Zăvoi [1], Alexandra Dreancă [1,2,*], Klara Magyari [2], Andrada Negoescu [1], Liviu Oana [1]

[1] University of Agricultural Sciences and Veterinary Medicine, Calea Mănăștur no 3-5, 400372, Cluj-Napoca, România; andreea-alina.zavoi@usamvcluj.ro; alexandra.dreanca@usamvcluj.ro; andrada.negoescu@usamvcluj.ro; liviu.oana@usamvcluj.ro;
[2] Nanostructured Materials and Bio-Nano-Interfaces Center, Interdisciplinary Research Institute on Bio-Nano-Sciences, Babes-Bolyai University, T. Laurian 42, 400271 Cluj-Napoca, Romania; klara.magyari@ubbcluj.ro;
* Correspondence: alexandra.dreanca@usamvcluj.ro

Abstract: Unlike minor muscle injuries, which can heal through the activation of resident satellite cells, VML injuries involve the removal of large tissue volumes and disruption of the extracellular matrix architecture required for effective regeneration. Consequently, the healing process is often dominated by fibrosis, chronic inflammation, and incomplete muscle regeneration. To overcome these limitations, considerable attention has been directed toward the development of biomimetic scaffolds and regenerative therapies designed to restore both the structural organization and functional properties of skeletal muscle. Understanding the histopathological lesions associated with VML is therefore crucial for assessing tissue repair and for developing effective treatment strategies capable of improving muscle recovery and functional outcomes.

Keywords: volumetric muscle loss; immunohistochemistry; rats.

Received: 16.06.2026
Accepted: 24.06.2026
Published: 25.06.2026

DOI:10.52331/v31i3dw89

Copyright: © 2021 by the authors. Submitted for possible open access publication under the terms and conditions of the Creative Commons Attribution (CC BY) license (http://creativecommons.org/licenses/by/4.0/).

1. Introduction

Severe skeletal muscle loss can occur in a variety of clinical contexts, including traumatic injuries, congenital conditions, surgical resections, and degenerative myopathies. Volumetric muscle loss (VML) is defined as the loss of skeletal muscle tissue that exceeds the endogenous regenerative capacity of the tissue, leading to incomplete structural and functional recovery [1,2]. Although skeletal muscle has a strong intrinsic ability to regenerate following minor injuries through satellite cell activation and coordinated repair mechanisms [3,4], extensive defects such as VML often result in persistent deficits in muscle architecture and function.

Current therapeutic approaches for VML primarily involve surgical reconstruction techniques, such as muscle flap transfers or autologous grafting procedures. However, these strategies are limited by donor-site morbidity, restricted availability of suitable tissue, and incomplete restoration of full muscle function. As a result, there has been increasing interest in the development of regenerative and tissue-engineering-based alternatives aimed at improving functional recovery [5-7].

Recent advances have focused on the design of biomimetic and tissue-engineered constructs, including scaffold-free, multi-phasic skeletal muscle units intended to restore both structural organization and contractile capacity. These engineered constructs often integrate muscle tissue with supportive anchoring structures to better replicate native musculoskeletal architecture. Preclinical evaluation of such therapies is commonly performed using rat models of VML, particularly involving injuries to the tibialis anterior (TA) muscle [8,9].

Despite widespread use of animal models, there remains significant variability in experimental design, including differences in species, injury geometry, and percentage of muscle removed. Common approaches include longitudinal excisions, transverse resections, and biopsy punch injuries, all of which typically exceed the regenerative threshold of skeletal muscle [10]. However, the degree of long-term functional impairment varies across studies, and recent findings suggest that some injury sizes previously considered representative of VML may still allow substantial recovery over extended time periods [11,12].

Consequently, there is a need to refine and standardize VML models to better reflect clinically relevant, long-lasting functional deficits. This includes systematic evaluation of different defect sizes and their long-term outcomes in order to identify injury thresholds that result in irreversible loss of muscle function. Such standardized models are essential for improving the comparability of studies and for the reliable assessment of emerging regenerative therapies [13].

The aim of this study was to evaluate the histological response of volumetric muscle loss defects treated with two bioactive glass-based biomaterials, bioactive glass-alginate-agarose (BG-Alg-Agar) and bioactive glass-agarose (BG-Agar), in a rat tibialis anterior model. A standardized full-thickness muscle defect corresponding to approximately 20% of muscle mass was surgically induced and subsequently treated with the biomaterials or left untreated as a control. Animals were euthanized at 4-, 6-, 8-, and 12-weeks post-implantation for histological and immunohistochemical evaluation.

Histological examination revealed progressive muscle regeneration in the treated groups, characterized by the appearance of centrally nucleated regenerating fibers, neovascularization, and active mesenchymal proliferation. Immunohistochemical analysis demonstrated sustained myogenic activity, particularly in the BG-Alg-Agar group, where muscle maturation and tissue organization improved over time. In contrast, BG-Agar-treated defects showed a less favorable regenerative outcome, with gradual replacement of the defect area by fibrous connective tissue and limited muscle fiber formation at later time points. Peri-implant calcifications were observed at 8 weeks in both biomaterial groups but regressed by 12 weeks, suggesting a temporary tissue response associated with remodeling rather than progressive pathological mineralization. Untreated defects exhibited persistent fibro-adipose tissue deposition and minimal evidence of muscle regeneration throughout the study period.

2. Materials and Methods

Twenty medium weighted males, Wistar rats, weighing 360 ± 50 g, were used for this experiment. Following the clinical examination, animals underwent a brief assessment of their general condition, including hydration status, appetite, and skin integrity. Both hindlimb surgical sites were aseptically prepared by shaving and disinfection, applied in concentric circular motions from the center outward. The limbs were draped under sterile conditions, with the right limb serving as an internal control. A longitudinal incision was made distal to the knee to expose the tibialis anterior (TA). Volumetric muscle loss was induced using a 6 mm biopsy punch, generating a full-thickness defect (~20% muscle mass) (Figure 1). Defects were filled with biomaterials (BG-Alg-Agar, n=10; BG-Agar, n=10) or left untreated as controls. Fascia and skin were continuously closed. This work was conducted in compliance with the European guidelines and rules 337, as established by the EU Directive 2010/63/EU and the Romanian law 43/2014. . As a biomaterial it was used sol-gel derived bioactive glass (BG; $60SiO_2{\cdot}32CaO{\cdot}8P_2O_5$ mol%) [14]. The BG was added in agarose (BG-Agar), and in alginate-agarose (BG-Alg-Agar) polymeric solutions in a ratio of 12 wt%. The weight ratio of alginate–agarose composite was 3:1 (Alg-Agar). All procedures were approved by the Research Ethics Committee of the University of Agricultural Sciences and Veterinary Medicine (USAMV) Cluj-Napoca, Romania, and they were authorised by the State Veterinary Authority (ethical approval number 369 /13.06.2023).

For microscopic analysis, tibialis anterior (TA) muscle samples were collected from both control and treated groups (BG-Alg-Agar and BG-Agar) at 4-, 6-, 8-, and 12- post-intervention. Specimens were fixed in 10% formalin for 24 h and processed using standard histological procedures. Paraffin-embedded tissues were sectioned at 3 μm using a Thermo Scientific™ Citadel 2000 rotary microtome and stained with hematoxylin and eosin (H&E).

For immunohistochemical analysis, heat-induced epitope retrieval was performed at pH = 9.0. using Novocastra™ Epitope Retrieval solution (1:10 dilution) for 30 minutes. Immunostaining was carried out using the Dako EnVision Flex+ (Mouse, high pH) system according to the manufacturer's instructions. Primary antibodies included anti-MyoD1 (ab203383, Abcam; 1:1000 dilution) and anti-α-smooth muscle actin (α-SMA, ab5694, Abcam; 1:100 dilution).

Slides were evaluated by two anatomical pathologists, and images were acquired using an Olympus SP-350 digital camera with Stream Basic imaging software (v1.5.1, Olympus Corporation, Tokyo, Japan).

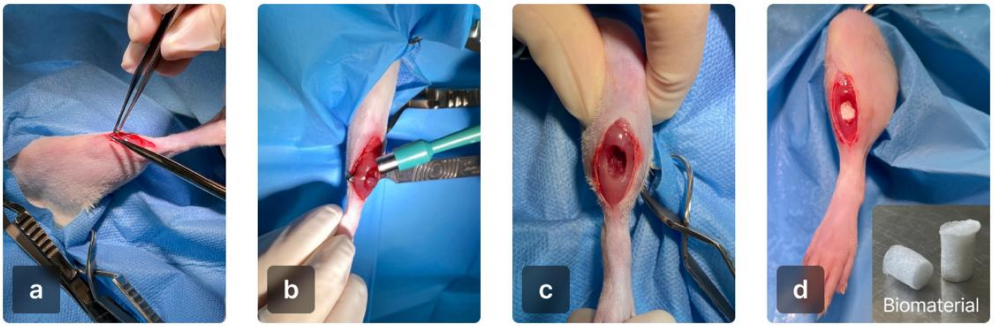

Figure 1. Schematic overview of VML surgery with BG-Alg-Agar and BG-Agar: (**a**) After shaving, skin and fascia were incised to expose the tibialis anterior muscle; (**b, c**) A 6 mm biopsy punch created a VML defect; (**d**) followed by hydrogel implantation or left untreated.

3. Results

Animals were euthanized by prolonged isoflurane anesthesia followed by cervical dislocation, and tibialis anterior (TA) muscles were harvested for analysis at 4-, 6-, 8-, and 12-weeks post-intervention.

3.1. Histologic features of fibrosis following VML injury

- BG-Alg-Agar group

At 4 weeks post-implantation, centrally nucleated muscle fibers indicate active regeneration. The tissue shows ongoing repair characterized by mesenchymal proliferation and inflammatory infiltration, predominantly macrophages involved in phagocytosis, without evidence of necrosis. However, tissue organization remains immature, with incomplete structural restoration and persistent but expected inflammatory activity (Figure 2a, b).

At 6 weeks, muscle fibers display staining patterns consistent with myoblastic activity, indicating continued but more advanced regeneration. The process is in an intermediate stage, with overlap between proliferation and differentiation. Inflammation is still present but shows signs of regression. The biomaterial is integrating into the tissue; however, focal dystrophic mineralization suggests a low-grade chronic inflammatory response. Mesenchymal activity persists, contributing to tissue remodeling, but regeneration remains incomplete and not fully physiological (Figure 2c, d).

At 8 weeks postoperatively, the defect region shows muscle fibers at an advanced stage of maturation, with increased diameter, peripheral nuclei, and improved cytoplasmic organization. These fibers are separated by thin connective tissue septa. Muscle regeneration is accompanied by ongoing but reduced neovascularization and partial integration of the biomaterial within the host tissue, which supports cellular migration and mesenchymal activity. However, remodeling remains incomplete, as evidenced by focal peri-implant calcifications and residual connective tissue deposition. These calcifications appear as dense basophilic deposits located between muscle fibers and within interstitial spaces, likely reflecting ongoing tissue remodeling and low-grade inflammatory activity (Figure 3a, b).

At 12 weeks, regenerated muscle fibers are uniformly aligned with peripheral nuclei and well-developed perimysial and endomysial organization. Tissue architecture shows marked improvement compared with earlier time points, although complete restoration of native skeletal muscle structure is not achieved. Low-grade inflammatory infiltrates and sparse calcifications persist, along with thin connective tissue septa between fibers, indicating residual remodeling activity. Mesenchymal proliferation is markedly reduced, reflecting transition toward tissue stabilization and maturation. The previously observed calcifications are now only sporadically present, suggesting a transient process. The biomaterial shows progressive resorption, contributing to consolidation of the regenerated tissue architecture (Figure 3c, d).

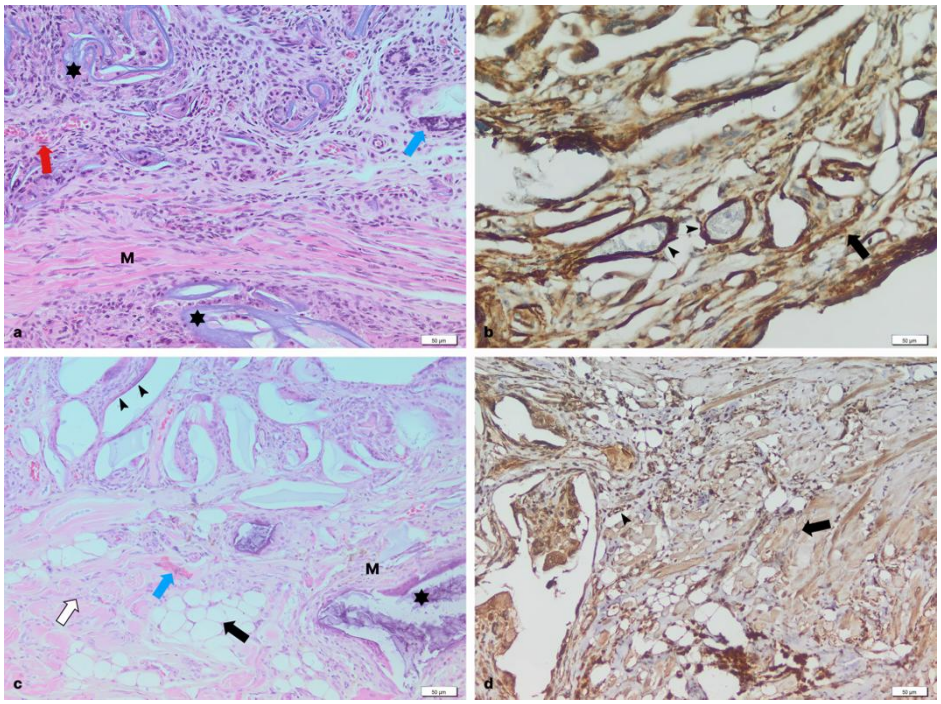

Figure 2. Histological evaluation of the tissue response in muscle defects at (**a, b**) 4 and (**c, d**) 6 weeks postoperatively in rats from the treated group. The defect is occupied by fragments of implanted material (black asterisk), surrounded by mesenchymal cells, blood vessels (blue arrow), collagen fibers, and mononuclear inflammatory cells; (**c**; arrowheads) Multinucleated myotubes are present at the periphery of the implant (red and white arrows), indicating ongoing myogenic activity; (**a, b**) Heterotopic bone formation with osteoblast rimming is also observed, H&E staining; (**b, d**; arrowheads) Immunohistochemistry shows vascular structures consistent with active angiogenesis and (**b, d**; black arrow) identifies positively stained myofibroblasts. Scale bars: (a,c) 100 μm and (b,d) 50 μm.

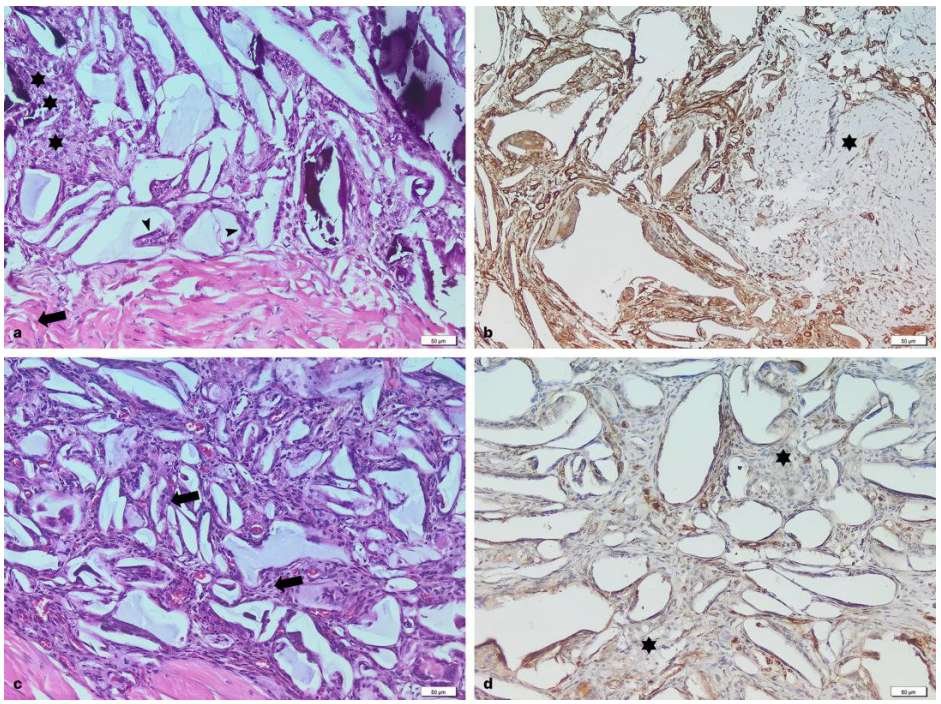

Figure 3. Histological evaluation of the tissue response in muscle defects at (**a, b**) 8 and (**c, d**) 12 weeks postoperatively in rats from the treated group. The defect area shows progressive tissue maturation characterized by reduced cellularity and predominance of remodeled connective tissue. Adipose infiltration and stabilized blood vessels are present, indicating ongoing tissue remodeling; (**a,**

c; black arrows) The inflammatory response is reduced compared with earlier stages; (**a**; arrowheads) Focal peri-implant hypertrophic calcifications are observed; (**a, c**) H&E staining. Immunohistochemistry shows organized extracellular matrix with reduced vascular density, consistent with late-stage tissue remodeling (asterisk). (a-d) Scale bar: 50 μm.

- BG-Agar group

At 4 weeks post-implantation, the muscle tissue consists of small fibers with centrally located nuclei, consistent with immature myotubes and early-stage regeneration. The defect area shows active and well-regulated repair, characterized by a predominant macrophage population involved in phagocytic clearance of cellular debris. Mesenchymal proliferation is evident, contributing to initial tissue restoration. The biomaterial remains present and may influence local diffusion and cellular activity. Overall, the histological pattern indicates an immature repair process without evidence of robust muscle reconstruction (Figure 4a, b).

At 6 weeks, muscle fibers show increased organization, although focal disruption and interstitial collagen deposition indicate early fibrotic remodeling. This suggests a transition toward a fibrotic repair trajectory that may limit further muscle regeneration despite ongoing mesenchymal activity. No active myofibroblasts are observed, and tissue remodeling appears limited, consistent with a transitional stabilization phase. Macrophages remain the dominant inflammatory cell population, reflecting low-grade chronic inflammation. The biomaterial demonstrates progressive integration into the host tissue, potentially accompanied by mild dystrophic mineralization, while mesenchymal proliferation persists at a reduced level, supporting residual reparative activity (Figure 4c, d).

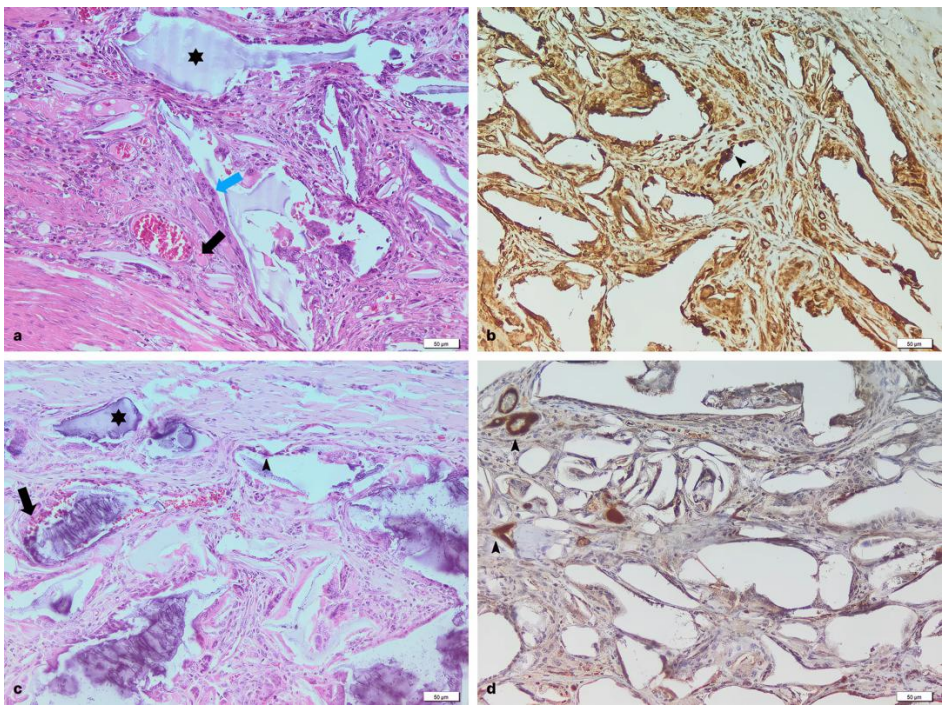

Figure 4. Histological evaluation of tissue response in muscle defects at (**a, b**) 4 and (**c, d**) 6 weeks postoperatively in the treated group. The muscle defect is occupied by fragments of the implanted material (black asterisk); (**a**, blue arrow) Immature myotubes are present; (**a, c**; black arrow) Presence of macrophages; (**c**; arrowhead) Mineralization; (**a, c**) H&E staining; (**b, d**; arrowheads) Immunohistochemical staining highlights vascular structures and confirms active angiogenesis in the tissue. (a, b, c, and d) Scale bar: 50 μm.

At 8 weeks, histological examination demonstrated incomplete muscle regeneration characterized by disorganized fibers, irregular alignment, increased connective tissue deposition, and expanded interstitial spaces. These features suggest a progressive shift toward fibrotic remodeling rather than functional muscle restoration. Immunohistochemical analysis (Figure 5a, b) revealed marker expression within the regenerated

tissue; however, staining was heterogeneous, with variable intensity and areas of reduced immunoreactivity, indicating uneven tissue maturation.

At 12 weeks, muscle fibers exhibited improved organization and a more compact architecture compared with earlier time points. Nevertheless, focal connective tissue persistence and irregular fiber arrangement remained, indicating incomplete remodeling. Immunohistochemical staining (Figure 5c, d) showed continued marker expression within regenerated tissue, but with non-uniform intensity across regions. These findings indicate progressive regeneration without full structural or functional maturation. Despite partial improvement in tissue organization, residual fibrotic areas and heterogeneous immunoreactivity suggest that skeletal muscle regeneration remained incomplete, with fibrotic remodeling still contributing to the overall tissue architecture.

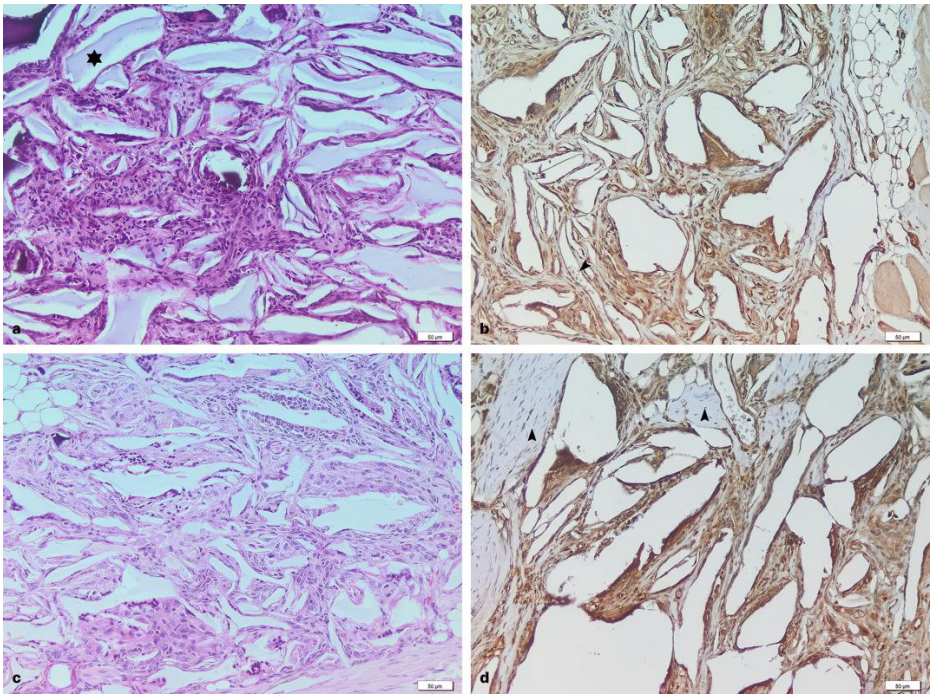

Figure 5. Histological evaluation of tissue response in muscle defects at (**a, b**) 8 and (**c, d**) 12 weeks postoperatively in the treated group. At 8 weeks, reduced and localized muscle fibers with occasional MyoD-positive cells are observed, indicating ongoing but limited regeneration. Inflammation is reduced, and partial biomaterial resorption is evident (black asterisk). At 12 weeks, muscle fibers are scarce and the defect is largely replaced by fibrous tissue, with complete biomaterial resorption and absence of active regeneration; (**a, c**) H&E staining; (**b, d**) Immunohistochemistry shows heterogeneous positive staining with variable intensity across regions (arrowheads). Scale bar: 50 µm.

- Control group

At 4 weeks postoperatively, the defect area showed neovascularization and active mesenchymal proliferation, indicating an early reparative response. The muscle defect was partially filled with fibro-adipose tissue composed of sparse fibroblasts, thick collagen fibers, and differentiated adipocytes, with limited neovascularization. At the interface with residual skeletal muscle, occasional myotubes were observed, indicating minimal regenerative activity (Figure 6a). *From 6 to 12 weeks*, the histological appearance of the defect remained largely unchanged. The lesion was consistently occupied by fibro-adipose tissue with vascular structures, without evidence of meaningful skeletal muscle regeneration. Occasional inflammatory lesions persisted, while new muscle fiber formation was absent or minimal throughout the observation period (Figure 6b).

Overall, untreated defects failed to regenerate functional skeletal muscle, with fibro-adipose tissue replacement representing the predominant healing response throughout the study period.

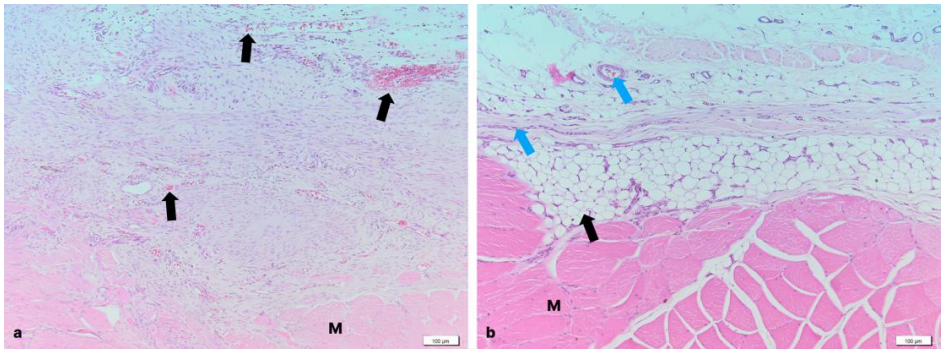

Figure 6. Histological evaluation of the tissue response in muscle defects at (a) 4 weeks and (b) 6, 8, and 12 weeks postoperatively in rats from the control group. *M* indicates skeletal muscle. (a, black arrows). Blood vessel formation can be observed. (b, black arrow) The presence of adipose tissue and blood vessels (blue arrows - b) is also noted. (a,b) H&E staining. The scale bar represents 100 μm.

3.2 Comparative histological outcomes of the investigated biomaterials

The histopathological evaluation demonstrated that both biomaterials were capable of supporting an initial regenerative response following volumetric muscle loss. However, neither scaffold achieved complete restoration of normal skeletal muscle architecture during the experimental period. The regenerative process remained heterogeneous and was accompanied by varying degrees of connective tissue deposition, indicating that the biological response was only partially successful.

Among the two investigated biomaterials, BG-Alg-Agar exhibited the most favorable regenerative profile. Histological examination revealed active myogenesis, angiogenesis, and mesenchymal cell proliferation during the early stages of healing, followed by progressive tissue organization and biomaterial integration. Nevertheless, complete muscle regeneration was not achieved, as residual connective tissue, persistent low-grade inflammation, and transient peri-implant calcifications were still evident at later time points. These findings suggest that although BG-Alg-Agar provided a supportive microenvironment for muscle repair, additional optimization of its composition or biological activity may be necessary to obtain complete structural recovery.

In contrast, the BG-Agar biomaterial demonstrated a less favorable histological outcome. While early regenerative activity was observed after implantation, the repair process progressively shifted toward fibrotic tissue formation, with irregular muscle fiber organization and persistent connective tissue deposition. The heterogeneous immunohistochemical staining pattern and incomplete maturation of regenerating fibers indicated limited myogenic potential, suggesting that this biomaterial alone was insufficient to sustain effective long-term skeletal muscle regeneration.

Despite these limitations, both biomaterials promoted a more organized reparative response than the untreated defects, in which fibro-adipose tissue predominated and muscle regeneration remained minimal throughout the observation period. The overall histological findings indicate that the regenerative capacity of the investigated scaffolds remains incomplete, emphasizing the need for further improvements in biomaterial design, degradation kinetics, and biological functionalization to enhance muscle regeneration and reduce fibrosis.

4. Discussion

Pathological fibrosis negatively affects skeletal muscle function by increasing tissue stiffness and reducing contractile capacity. In the context of volumetric muscle loss, early post-injury healing is characterized by transient extracellular matrix remodeling, including elevated collagen type III deposition and a loosely organized matrix within the defect area, reflecting an initial reparative phase [15].

A key finding of this study is the occurrence of transient heterotopic calcification within the implant region. Although ectopic mineralization is generally considered an undesirable outcome in regenerative therapies, the temporal pattern observed (presence at 8 weeks followed by regression at 12 weeks) suggests that these deposits are associated with active tissue remodeling rather than progressive pathological ossification [17-19]. Similar transient mineralization phenomena have been reported in biomaterial implantation studies and are frequently linked to local ionic fluctuations, macrophage-mediated inflammatory responses,

and extracellular matrix remodeling [20]. However, the mechanisms underlying this phenomenon in the present model were not investigated in detail and require further analysis using dedicated imaging modalities and mineral-specific histological techniques.

Immunohistochemical analysis using MyoD and α-SMA provided additional insight into the regenerative process. Sustained MyoD expression and the presence of regenerating fibers indicate prolonged myogenic activity, particularly in the BG-Alg-Agar group. MyoD is a key regulator of satellite cell activation and myogenic differentiation, and its expression is generally associated with active muscle repair [21]. The persistence of MyoD-positive cells at intermediate stages suggests that the regenerative process remains active beyond the acute injury phase, consistent with previous studies reporting prolonged myogenic responses in successfully regenerating VML defects treated with biomaterials [22].

Despite these regenerative signals, the histopathological assessment was primarily qualitative and lacked extensive histomorphometric quantification of fibrosis, vascularization, and muscle regeneration. In addition, a broader panel of molecular markers was not employed to fully characterize inflammatory and fibrotic pathways, limiting mechanistic interpretation.

Future studies should focus on a multifaceted optimization strategy. From a biomaterials perspective, tuning composition, degradation kinetics, surface chemistry, porosity, and ion exchange properties may reduce local conditions favoring ectopic mineralization and excessive inflammatory signaling. From a biological standpoint, modulation of macrophage polarization and inhibition of osteogenic signaling pathways may further improve regenerative outcomes and limit calcification [24,25].

More clinically relevant preclinical models, such as rabbits, pigs, or sheep, may provide improved translational relevance due to their closer approximation of human muscle architecture, vascularization, and mechanical loading conditions [23]. These models may better capture tissue remodeling dynamics and susceptibility to heterotopic ossification.

Clinically, heterotopic ossification remains a relevant complication in muscle injuries, particularly those adjacent to bone. It has been reported in up to 20% of patients following muscle contusion injuries and in up to 65% of cases of traumatic volumetric muscle loss [27-29].

5. Conclusions

Overall, the findings indicate that BG-Alg-Agar provides a more favorable regenerative microenvironment than BG-Agar, supporting early myogenic activity, angiogenesis, and biomaterial integration, while partially limiting fibrotic progression. However, neither scaffold achieved complete restoration of native skeletal muscle architecture within the 12-week period. Persistent connective tissue deposition and transient peri-implant calcifications indicate that tissue remodeling remained incomplete at the study endpoint. Although bioactive glass-based composite scaffolds show promise for volumetric muscle loss repair, further optimization of their physicochemical and biological properties is required to enhance functional muscle regeneration and reduce fibrotic healing outcomes. Future studies should incorporate quantitative histomorphometric and functional assessments, as well as larger animal models, to improve translational relevance. Local anatomical conditions may also influence regenerative outcomes, particularly in muscle defects adjacent to bone, where altered mechanical and biochemical microenvironments may shift the balance between muscle regeneration, fibrosis, and ectopic mineralization.

Author Contributions: Conceptualization, A.M, A.D. and K.M.; methodology, A.D and K.M.; validation, A.D.; methodology and investigation, A.N and K.M.; writing - original draft preparation, A.M. and A.D.; writing - review and editing, K.M. and A.D.; validation and supervision, L.O.; project administration, L.O. All authors have read and agreed to the published version of the manuscript.

Funding: This research received no external funding

Institutional Review Board Statement: This work was conducted in compliance with the European guidelines and rules 337, as established by the EU Directive 2010/63/EU and the Romanian law 43/2004. All procedures were approved by the Research Ethics Committee of the University of Agricultural Sciences and Veterinary Medicine (USAMV) Cluj-Napoca, Romania, and they were authorized by the State Veterinary Authority (number 369/13.06.2023)

Conflicts of Interest: The authors declare no conflict of interest.

References

1. Garg, K., Brockhouse, J., McAndrew, C.M., Reiter, A.J., Owens, J.G., Mueller, R.J., Pena, G., Ridolfo, A. and Johnson, D.L., Regenerative rehabilitation: Navigating the gap between preclinical promises and clinical realities for treating trauma-induced volumetric muscle loss. *J Physiol* **2025**, *603*, 7421-7439.
2. Corona, B. T., Wenke, J. C., Ward, C. L. Pathophysiology of volumetric muscle loss injury. *Cells Tissues Organs* **2016**, *202(3-4)*, 180-188.
3. Tang, X., Daneshmandi, L., Awale, G., Nair, L.S., Laurencin, C.T. Skeletal Muscle Regenerative Engineering. *Regen Eng Transl Med* **2019**, *5*(*3*), 233-251.
4. Garg, K., Ward, C. L., Hurtgen, B. J., Wilken, J. M., Stinner, D. J., Wenke, J. C., Owens J.G., Corona, B. T. Volumetric muscle loss: persistent functional deficits beyond frank loss of tissue. *J Orthop Res* **2015**, *33(1*), 40-46.
5. Shayan, M., Huang, N.F. Pre-Clinical Cell Therapeutic Approaches for Repair of Volumetric Muscle Loss. *Bioeng* **2020**, *7*, 97.
6. Eugenis, I., Wu, D., Rando, T.A. Cells, scaffolds, and bioactive factors: Engineering strategies for improving regeneration following volumetric muscle loss. *Biomaterials* **2021**, *278*, 121173.
7. Shayan, M., Huang, N.F. Pre-Clinical Cell Therapeutic Approaches for Repair of Volumetric Muscle Loss. *Bioengineering (Basel)* **2020**, 20, *7(3)*, 97.
8. Cittadella Vigodarzere, G., Mantero, S. Skeletal muscle tissue engineering: strategies for volumetric constructs. *Front Physiol* **2014**, *22(5),* 362.
9. Rodriguez, B. L., Florida, S. E., VanDusen, K. W., Syverud, B. C., Larkin, L. M. The maturation of tissue-engineered skeletal muscle units following 28-day ectopic implantation in a rat. *Regen Eng Transl Med* **2019**, *5(1)*, 86-94.
10. Sicherer, S.T., Venkatarama, R.S., Grasman, J.M. Recent Trends in Injury Models to Study Skeletal Muscle Regeneration and Repair. *Bioengineering* (Basel) **2020**, 20, *7(3)*, 76.
11. Greising, S.M., Dearth, C.L., Corona, B.T. Regenerative and Rehabilitative Medicine: A Necessary Synergy for Functional Recovery from Volumetric Muscle Loss Injury. *Cells Tissues Organs* **2016**, *202(3-4)*, 237-249.
12. Testa, S., Fornetti, E., Fuoco, C., Sanchez-Riera, C., Rizzo, F.; Ciccotti, M., Cannata, S., Sciarra, T., Gargioli, C. The War after War: Volumetric Muscle Loss Incidence, Implication, Current Therapies and Emerging Reconstructive Strategies, a Comprehensive Review. *Biomedicines* **2021**, *9*, 564.
13. Wu, X., Corona, B.T., Chen, X., Walters, T.J. A standardized rat model of volumetric muscle loss injury for the development of tissue engineering therapies. *Biores Open Access* **2012**, *1(6)*, 280-90.
14. Magyari, K., Baia, L., Vulpoi, A., Simon, S., Popescu, O., Simon, V. Bioactivity evolution of the surface functionalized bioactive glasses. *J Biomed Mater Res B Appl Biomater* **2015**, *103(2)*, 261-72.
15. Dolan, C.P., Motherwell, J.M., Franco, S.R., Janakiram, N.B., Valerio, M.S., Goldman, S.M., Dearth. C.L. Evaluating the potential use of functional fibrosis to facilitate improved outcomes following volumetric muscle loss injury. *Acta Biomater* **2022**, *140*, 379-388.
16. Meyers, C., Lisiecki, J., Miller, S., Levin, A., Fayad, L., Ding, C., Sono, T., McCarthy, E., Levi, B., James, A.W. Heterotopic Ossification: A Comprehensive Review. *JBMR Plus* **2019**, 27, *3(4)*:e10172.
17. Li, Q., Jiang, Q., Uitto, J. Ectopic mineralization disorders of the extracellular matrix of connective tissue: molecular genetics and pathomechanisms of aberrant calcification. *Matrix Biol.* **2014**, *33*, 23-8.
18. Song, J.H., Liu, M.Y., Ma, Y.X., Wan, Q.Q., Li, J., Diao, X.O., Niu, L.N. Inflammation-associated ectopic mineralization. *Fundam Res* **2022**, *3(6)*, 1025-1038.
19. Giachelli, C.M. Ectopic calcification: gathering hard facts about soft tissue mineralization. *Am J Pathol.* **1999**, *154(3)*, 671-5.
20. Frumento, D.; Ţălu, Ş. Advanced Coating Strategies for Immunomodulatory Biomaterials for Reconstructive Osteogenesis: Mitigating Foreign Body Reaction and Promoting Tissue Regeneration. *Coat* **2025**, *15*, 1026.
21. Careccia, G., Mangiavini, L., Cirillo, F. Regulation of Satellite Cells Functions during Skeletal Muscle Regeneration: A Critical Step in Physiological and Pathological Conditions. *Int J Mol Sci* **2023**, *25(1)*, 512.
22. Tanner, G.I., Schiltz, L., Narra, N., Figueiredo, M.L., Qazi, T.H. Granular Hydrogels Improve Myogenic Invasion and Repair after Volumetric Muscle Loss. *Adv Healthc Mater* **2024**, *13(25)*, e2303576.
23. Rao, Y., Saiz-Gonzalo, G., Prateeksha, P., Wang, A., Shi, H., Wang, W., Li, C. Selection of experimental animals and modeling methods in developmental dysplasia of the hip research. *EFORT Open Rev* **2025**, *10(7)*, 496-509.
24. Ten Brink, T., Damanik, F., Rotmans, J.I., Moroni, L. Unraveling and Harnessing the Immune Response at the Cell-Biomaterial Interface for Tissue Engineering Purposes. *Adv Healthc Mater* **2024**, *13(17)*, e2301939.
25. Li, J., Xie, J., Wang, Y., Li, X., Yang, L., Zhao, M., Chen, C. Development of Biomaterials to Modulate the Function of Macrophages in Wound Healing. *Bioeng* **2024**, *11*, 1017.
26. Järvinen, T.A. Neovascularisation in tendinopathy: from eradication to stabilisation? *Br J Sports Med* **2020**, *54(1)*, 1-2.
27. Beiner, J.M., Jokl, P. Muscle contusion injury and myositis ossificans traumatica. *Clin Orthop Relat Res* **2002**, *403* Suppl: S110-9.
28. King, J.B. Post-traumatic ectopic calcification in the muscles of athletes: a review. *Br J Sports Med* **1998**, *32(4)*, 287-90.
29. Forsberg, J.A., Pepek, J.M., Wagner, S., Wilson, K., Flint, J., Andersen, R.C., Tadaki, D., Gage, F.A., Stojadinovic, A., Elster, E.A. Heterotopic ossification in high-energy wartime extremity injuries: prevalence and risk factors. *J Bone Joint Surg Am* **2009**, *91*(5), 1084-91.